Intraventricularly Injected Olig2-NSCs Attenuate Established Relapsing-Remitting EAE in Mice

Sher, Falak; Amor, Sandra; Gerritsen, Wouter; Baker, David; Jackson, Samuel L.; Boddeke, Erik; Copray, Sjef

Published in:
Cell Transplantation

DOI:
10.3727/096368911X637443

Cell Transplantation, Vol. 21, pp. 1883–1897, 2012

0963-6897/12 $90.00 + .00
DOI: http://dx.doi.org/10.3727/096368911X637443
E-ISSN 1555-3892
www.cognizantcommunication.com

Intraventricularly Injected Olig2-NSCs Attenuate Established Relapsing–Remitting EAE in Mice

Falak Sher,* Sandra Amor,†‡ Wouter Gerritsen,† David Baker,‡ Samuel L. Jackson,‡ Erik Boddeke,* and Sjef Copray*

*Department of Neuroscience, University Medical Centre Groningen, Groningen, The Netherlands
†Department of Pathology, VU University Medical Centre, Amsterdam, The Netherlands
‡Department of Neuroscience and Trauma Centre, Barts and the London School of Medicine and Dentistry, Queen Mary University of London, London, UK

In multiple sclerosis (MS), a chronic inflammatory relapsing demyelinating disease, failure to control or repair damage leads to progressive neurological dysfunction and neurodegeneration. Implantation of neural stem cells (NSCs) has been shown to promote repair and functional recovery in the acute experimental autoimmune encephalomyelitis (EAE) animal model for MS; the major therapeutic mechanism of these NSCs appeared to be immune regulation. In the present study, we examined the efficacy of intraventricularly injected NSCs in chronic relapsing experimental autoimmune encephalomyelitis (CREAE), the animal disease model that is widely accepted to mimic most closely recurrent inflammatory demyelination lesions as observed in relapsing–remitting MS. In addition, we assessed whether priming these NSCs to become oligodendrocyte precursor cells (OPCs) by transient overexpression of Olig2 would further promote functional recovery, for example, by contributing to actual remyelination. Upon injection at the onset of the acute phase or the relapse phase of CREAE, NSCs as well as Olig2-NSCs directly migrated toward active lesions in the spinal cord as visualized by in vivo bioluminescence and biofluorescence imaging, and once in the spinal cord, the majority of Olig2-NSCs, in contrast to NSCs, differentiated into OPCs. The survival of Olig2-NSCs was significantly higher than that of injected control NSCs, which remained undifferentiated. Nevertheless, both Olig2-NSCs and NSC significantly reduced the clinical signs of acute and relapsing disease and, in case of Olig2-NSCs, even completely abrogated relapsing disease when administered early after onset of acute disease. We provide the first evidence that NSCs and in particular NSC-derived OPCs (Olig2-NSCs) ameliorate established chronic relapsing EAE in mice. Our experimental data in established neurological disease in mice indicate that such therapy may be effective in relapsing–remitting MS preventing chronic progressive disease.

Key words: Oligodendrocyte; Remyelination; Multiple sclerosis

INTRODUCTION

Multiple sclerosis (MS) is one of the most common neuroimmunological disorders of the central nervous system (CNS). It is distinguished by multiple autoimmune inflammatory assaults in the CNS, resulting in oligodendrocyte impairment and/or degeneration, which lead to axonal demyelination, injury, and dysfunction. Whereas the development of anti-inflammatory drugs for MS has made significant progress in the last decades, strategies for remyelination and axonal restoration require further development and refinement. Importantly, developments in stem cell research, in particular the discovery of induced pluripotent stem (iPS) cells enabling the generation of infinite numbers of autologous neural stem cells (NSCs) (29), have revived the idea of cell-based therapy as an approach for inducing remyelination and, with that, the slowing or preventing of axonal degeneration. Unprecedently, a potentially clinicaly relevant source for transplantable remyelinating cells has become within reach.

Indeed, endogenous NSCs residing in specific germinal niches in the CNS are thought to produce new oligodendrocyte precursor cells (OPCs) and so to contribute to myelin repair after a demyelinating assault. However, the efficacy of these endogenous NSCs in contributing to myelin repair is limited (for a review, see 24). Transplantation of exogenous NSCs signifies an alternative and potentially more efficient therapeutic approach to accomplish remyelination in MS. A number of studies in the acute experimental autoimmune encephalomyelitis (EAE) mouse model for MS (for a review, see 7)

Received March 9, 2011; final acceptance October 29, 2011. Online prepub date: March 28, 2012.
Address correspondence to Dr. Sjef Copray, Department of Neuroscience, University Medical Centre Groningen, A. Deusinglaan 1, 9713 AV Groningen, The Netherlands. Tel: +31 50 3632785; Fax: +31 50 3632751; E-mail: j.c.v.m.copray@med.umcg.nl

have shown that NSCs indeed have a beneficial effect after grafting and significantly reduced clinical scores. Recently, human neural stem cells were administered to nonhuman primates in which EAE was induced and similar observations were made (23). However, the beneficial effect on acute EAE symptoms appeared not (or at least not directly) to be achieved by promotion of remyelination but by the reduction of inflammation via various trophic, immunomodulatory, and even T-cell apoptosis-inducing factors produced by the undifferentiated NSCs (11–13,24–27). These studies reveal that grafted undifferentiated NSCs, although optimally equipped for homing to the lesions, show only marginal differentiation into remyelinating oligodendrocytes at the site of the lesion. In a previous study, we have primed NSCs toward an oligodendrocyte cell lineage by the induced overexpression of Olig2 (9) before transplanting them into the demyelinated corpus callosum of cuprizone-fed mice to induce chronic demyelination (31). We compared the long-term survival and functional behavior of these Olig2-NSCs with implanted undifferentiated NSCs and found that, in contrast to undifferentiated NSCs, Olig2-NSCs survived and developed into myelinating oligodendrocytes contributing to the remyelination of the corpus callosum (31). Recently, a similar approach with human NSCs was successful in transplantation experiments in the lesioned white matter of rat spinal cord, namely, that grafted human Olig2-NSCs, in contrast to undifferentiated NSCs, significantly aided remyelination and promoted locomotor recovery (17).

Obviously, the conditions in the demyelination lesions in the animal models mentioned above are not comparable to the inflammatory conditions in demyelination lesions in relapsing–remitting MS; the presence of reactive T cells, monocytes, macrophages, activated microglia, and astrocytes as well as the proinflammatory milieu of, for example, cytokines and chemokines produced by these cells, may affect the migration, survival, and remyelination activity of implanted NSCs and Olig2-NSCs.

Therefore, in the present study, we have investigated the survival, migration, and functional behavior of NSCs as well as Olig2-NSCs after intraventricular injection in a chronic inflammatory model of MS, the chronic relapsing EAE mouse, the animal disease model, which is widely accepted to sufficiently mimic inflammatory demyelination lesions as observed in MS.

MATERIALS AND METHODS

Animals

The EAE implantation experiments were performed in 8- to 10-week-old female FVB ($n=32$) and Biozzi ABH ($n=24$) mice supplied by Harlan (Harlan, Horst, The Netherlands; http://www.harlan.com/about_harlan_laboratories). In addition, we have used FVB luciferase-green fluorescent protein (GFP)-actin transgenic mice (kindly donated by Christopher Contag, Stanford University, San Francisco, CA, USA) for the isolation of luciferase-GFP-positive NSCs. All mice were housed under standard conditions with free access to food and water. All animal experiments were designed and carried out in accordance with the National Institutes of Health Guidelines for the Care and Use of Laboratory Animals and Regulations of the Local Experimental Animal Committee.

Experimental Autoimmune Encephalomyelitis (EAE)

FVB Mice. Female FVB mice were injected subcutaneously with a sonicated emulsion consisting of 200 μg human recombinant myelin-oligodendrocyte glycoprotein (MOG) 35–55 emulsified in incomplete Freund's adjuvant (IFA) supplemented with 60 μg killed *Mycobacteria tuberculosis* on days 0 and 7 as described previously (1–4). Immediately and 24 h after immunization, the FVB mice were also injected IP with 200 ng of pertussis toxin, derived from *Bordetella pertussis* (Speywood, Porton Down, UK) dissolved in sterile water. In FVB mice, this induction protocol induces a monophasic acute form of EAE. EAE FVB mice were included in the experimental studies that started EAE symptoms within days 10–12 after immunization.

Biozzi ABH Mice. To examine the effects of NSC implantation in chronic relapsing–remitting EAE in which myelin damage is more prominent in the relapse phases (4), Biozzi ABH mice were used. The same immunization protocol was used as described above, in which lyophilized homologous spinal cord in phosphate-buffered saline (PBS, 0.1 M) replaced the MOG peptide. Animals were weighed daily and assessed for neurological signs from day 7 postinoculation. EAE Biozzi mice were included in the experimental studies with EAE symptoms starting within days 10–12 after immunization.

Signs of EAE were scored as follows: 0 = normal, 1 = limp tail, 2 = impaired righting reflex, 3 = partial hind-limb paralysis, 4 = total hind-limb paralysis, 5 = oribund (euthanized).

Neural Stem Cells (NSCs)

For potential future clinical application of NSCs, pluripotent sources like embryonic stem cells, in particular, induced pluripotent stem (IPS) cells, may be the source of choice for NSCs; such NSCs are not specifically proned for oligodendrocyte differentiation. Therefore, also in the present study, we have chosen to use E14 telencephalic NSCs, that is, NSCs that are not (yet) involved in oligodendrocyte formation. The NSCs were isolated from the brain of either luciferase-GFP-actin transgenic mouse embryos or Biozzi ABH embryos at embryonic day E14. Briefly, the brain was

cut into small pieces at room temperature, and following mechanical trituration in ice-cold phosphate-buffered saline (PBS, 0.1 M), small pieces of tissue were incubated with accutase (Sigma-Aldrich, St. Louis, MO, USA; http://www.sigmaaldrich.com) for 10 min at 37°C. After repeated trituration, the cell suspension was passed through a cell strainer (70 μm pore size; Falcon, Franklin Lakes, NJ, USA; http://www.bdbiosciences.com) and seeded (1–1.5 million cells) in T25 cm^2 tissue culture flasks (Nunc, Roskilde, Denmark; http://www.nuncbrand.com) containing proliferation medium, which consisted of neurobasal medium (Invitrogen, Breda, The Netherlands; http://www.invitrogen.com) supplemented with B27 (2%; Invitrogen), human recombinant epidermal growth factor (20 ng/ml; Invitrogen), basic fibroblast growth factor (20 ng/ml; Invitrogen), glutamax (1%; Invitrogen), primocin (100 μg/ml), and heparin (5 μg/ml; Sigma-Aldrich) in a humidified 5% CO_2/95% air incubator at 37°C. Luciferase expression in isolated and cultured NSCs isolated from luciferase-GFP-actin transgenic FVB mice was verified with a standard luciferase assay in a bioluminometer. The NSCs isolated from the ABH mice were labeled before implantation either by transfection of the firefly luciferase gene (see below) or by uptake of dragon green fluorophores (Bangs Laboratories, Inc., Fishers, IN, USA): 1.7 μl (approximately 5×10^6 particles) of fluorophores were added per milliliter of medium 24 h before the implantation of the cells. Labeling efficiency was approximately 90%.

Gene Transfection

Overexpression of Olig2 was induced in NSCs isolated from the luciferase-GFP transgenic FVB mice by transfection of an internal ribosome entry site plasmid (pIRES) expression vector containing the Olig2 gene; the parallel undifferentiated NSC group of FVB mice received a similar control transfection with GFP. NSCs isolated from Biozzi ABH mice were transfected with the same pIRES vector containing the firefly luciferase gene or the Olig2 gene. In both cases, transfection was performed using an Amaxa electroporation protocol (Amaxa GmbH, Cologne, Germany; http://www.amaxa.com) specifically designed for the transfection of embryonic mouse NSCs. The transfection efficiency of this procedure for mouse NSCs is approximately 85% and results in the transient expression of the transfected gene lasting up to 10–12 days.

Implantation of NSCs

FVB Mice. To examine the effect of NSC implantation in the acute phase of EAE, FVB mice were divided into three groups: group 1, received an injection at the first signs of acute EAE ($n = 10$); group 2, received an injection after recovering from the first episode of disease ($n = 8$); and group 3, the control group that was not EAE immunized ($n = 4$). Using a standard stereotactic procedure, half of the mice in groups 1 and 2 received an intraventricular injection of 1.5×10^5 NSCs while the other half received 1.5×10^5 Olig2-NSCs; stereotactic coordinates used (in relation to Bregma) anterior–posterior (−0.5), lateral (−1.0), and vertical (−2.6) according to the stereotaxic mouse brain atlas of Paxinos and Franklin (22). The mice in group 3 only received Olig2-NSCs. Sham mice ($n = 2$) were injected with only PBS.

Biozzi Mice. To examine the effects of NSC implants in the demyelinating relapsing–remitting form of EAE, EAE was induced in Biozzi ABH mice. Once clinical EAE was observed, the mice were randomly allocated into two groups: one group ($n = 8$) received an intraventricular implantation (same protocol as described above) at first signs of the primary acute attack, and the second group ($n = 6$) was injected intraventricularly at the onset of the first relapse. Similar to the EAE FVB mice, half of each group received 1.5×10^5 NSCs, while the other half received 1.5×10^5 Olig2-NSCs.

In Vivo Bioluminescence and Fluorescence Tracing of Implants

For the in vivo tracking of the luciferase-positive cell grafts, each animal was imaged three to four times per week with the use of the IVIS Imaging System 200 Series of Xenogen Corporation (Caliper Life Sciences, Alameda, CA, USA; http://www.caliperls.com). At each imaging session, each mouse received an IP injection of D-luciferin (300 mg/kg) in normal physiological salt solution. Ten minutes after the D-luciferin injection, animals were anesthetized with isoflurane (2.5% isoflurane in oxygen, 1.5 L/min) and placed in a standardized position in the chamber of a charge-coupled device camera system. The Dragon green-labeled cells were traced by using the fluorescein filter sets of the IVIS. The Living Image 2.5 software program (Xenogen Corporation, Caliper Life Sciences) was used for data analysis. Images representing luciferin and fluorescein light intensity, ranging from blue to red (for luciferase) and from black to yellow (fluorescein), were merged with the reference image to enable anatomical localization. Images were displayed, and regions of interest were quantified in terms of radiance [photons/s/cm^2/steradian (sr)].

Immunohistochemistry

At 8–10 days after implantation, that is, day 12 in the FVB and day 50 in the Biozzi mice**,** animals were perfused transcardially with 4% paraformaldehyde (PFA) under isoflurane anesthesia. In addition, as controls, EAE

mice that did not receive an implant were perfusion-fixed at various time points. Spinal cords were excised and sectioned on a cryostat. Sections were stained with cresyl violet for an overview of the pathology or stained with Luxol Fast Blue to examine myelin damage. Most of the tissues were used for immunohistochemistry. To identify luciferase-GFP or luciferase-labeled implanted cells, immunostaining was performed after heat-induced antigen/epitope retrieval (HIER) (10 mM sodium citrate, 0.05% Tween 20, pH 6.0) (required for luciferase immunostaining) using goat anti-luciferase (ab3256; Chemicon, Millipore, Amsterdam, The Netherlands; http://www.millipore.com) or rabbit anti-GFP (ab290; Abcam, Cambridge, MA, USA; http://www.abcam.com). To evaluate the survival and differentiation of the cell implants, the following primary antibodies directed against marker proteins specifically expressed by freshly differentiated oligodendrocytes, neurons, or astrocytes were used for astroblasts, anti-S100β (11420, 1:400; ICN Biomedicals, Inc., Irvine, CA, USA; http://www.mpbio.com) and anti-glial fibrillary acidic protein (GFAP) (mab3402; Millipore-Chemicon); for neuroblasts, anti-doublecortin (DCX) (AB5910, 1:500; Millipore-Chemicon); and for oligodendrocyte precursor cells, anti-RIP (mab1580; Millipore-Chemicon) or anti-NG2 (ab5320; Millipore-Chemicon). Subsequently, various fluorescent secondary antibodies were used to visualize the specific primary immunoreaction product in single and double immunohistochemical staining.

Chemotaxis Assay

NSCs and Olig2-NSCs migration in response to the chemokines CXCL12 [chemokine (C-X-C motif) ligand 12] and CXCL9 was assessed using a 48-well chemotaxis microchamber (Neuroprobe, AP48, Gaithersburg, MD, USA). A volume of 28 µl of chemokine solution (in neurobasal medium at concentrations of 10 nM) or control medium (neurobasal medium) was added to the lower wells. A total of 5×10^4 cells per 50 µl were used in the assay. The chamber was incubated at 37°C, 5% CO_2, in a humidified atmosphere for 4–5 h. After the incubation, the filter was fixed in Fast Green in 100% methanol with the concentration of 0.002 g/L (Diff-Quik Fix, Dade Behring, Düdingen, Fribourg, Switzerland) and stained twice, first in stain solution 1, containing 1.22 g/L eosin G in phosphatase buffer with the pH value of 6.6 (Diff-Quik), and then in stain solution 2, containing 1.1 g/L thiazine dye in phosphate buffer with pH 6.6. After staining, the filter membrane was cleaned on the upper side and dried. Migrated cells were counted with a scored eyepiece [3 fields (1 mm^2) per well], and migrated cells per chamber were calculated. The data are presented as percentages of control migration ± SEM and were analyzed by Student's *t* test. Control migration in response to neurobasal media is set to 100%. Values of $p < 0.05$ were considered significant.

RT-PCR

Total RNA was isolated from NSCs and Olig2-NSCs. Cells were lysed in guanidinium isothiocyanate/mercaptoethanol buffer, and RNA was extracted with phenol-chloroform and precipitated by using isopropanol. To degrade possible genomic DNA traces, DNase (Fermentis) was used. One microgram of total RNA was used for reverse transcriptase (RT) reaction and 2 µl of the RT reaction were used in subsequent PCR amplification using following primer pairs: chemokine (C-X-C motif) receptor 4 (CXCR4), sense 5′-TCCAAGGGCCACCAGAAGCG-3′, antisense 5′-AACTTGGCCCCGAGGAAGGC-3′; CXCR3, sense 5′-GCCAAGCCATGTACCTTGAGGTTAGT-3′, antisense 5′-AGGTGTCCGTGCTGCTCAGG-3′.

Cell Counting

Quantitative analysis of implanted cells was carried out by counting GFP^+ or dragon green $fluorophores^+$ cells in coronal cryostat sections of the spinal cord using a fluorescent microscope equipped with a Leica DFC300FX camera and the Leica microsystem LAS program (Leica, Heerbrugg, Switzerland; http://www.leica.com). The spinal cord was cut in three equal segments containing, respectively, the cervical, thoracic, and lumbar spinal cord. Every 10th section (14 µm) of this segment was collected and put on glass slides for immunofluorescent staining procedures. For each spinal segment, 10 subsequent sections were analyzed and used for cell counting. The number of cells in the spinal cord was calculated by the summation of the number of cells in each of the three spinal cord segments multiplied by a factor 10. Quantification of different cell types was performed based on cell type-specific double immunostaining (GFP or dragon green fluorophores/cell-specific marker). Statistical analysis of the results of all animals in each group was performed using Student's *t* test; values of $p < 0.05$ were considered significant.

RESULTS

EAE in FVB Mice Strain

Induction of EAE in the FVB mice results in an acute monophasic clinical course (Fig. 1A). The typical pattern of disease progress started at days 10–12 after immunization, with a peak at days 17–18 and a recovery that was almost complete by days 27–28. The arrows in Figure 1A indicate the time points of injection of the NSCs. The clinical signs in this monophasic acute form of EAE are the result of extensive inflammation with substantial cell infiltration (Fig. 1B) and edema formation in the spinal cord with

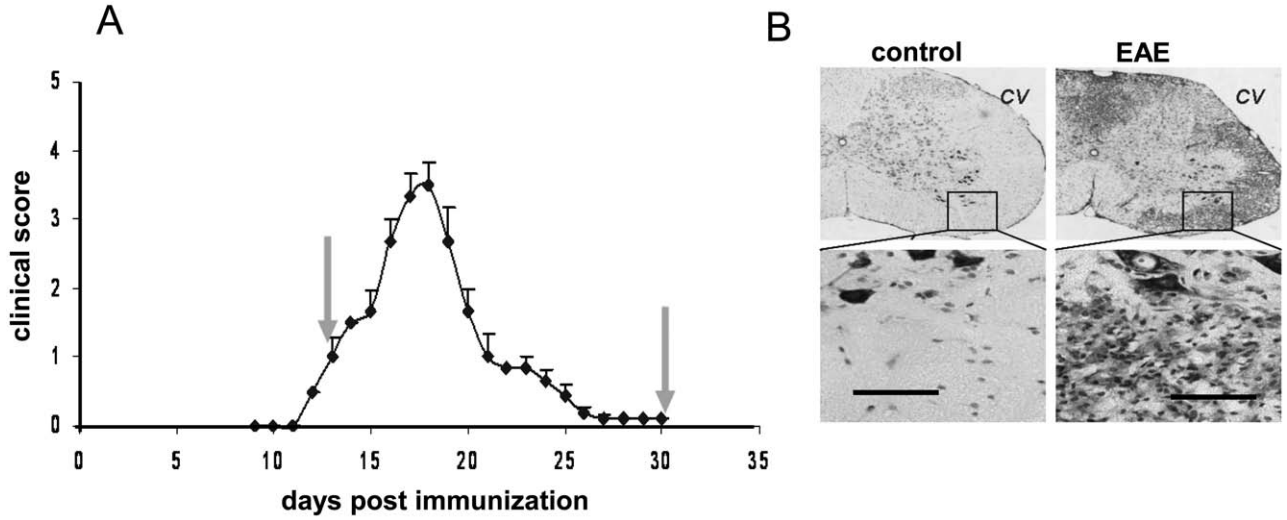

Figure 1. Experimental autoimmune encephalomyelitis (EAE) disease course in FVB mice. (A) The clinical scores of EAE in FVB mice ($n=10$; ±SEMs) reveal a clear monophasic pattern. The arrows indicate the time points of intraventricular injection of neural stem cells (NSCs) and Olig2-NSCs. (B) Sections of spinal cord stained for cresyl violet (CV) taken at peak of clinical score show extensive cellular infiltration in the funiculus white matter; compared with healthy control mice. Scale bar: 100 μm.

only minor contribution of demyelination and subsequent axonal injury.

Intraventricularly Injected Neural Stem Cells Migrate Only to Active EAE Lesions

Luciferase-labeled NSCs and luciferase-labeled Olig2-NSCs were implanted in the FVB mice intraventricularly, and their distribution and migration were monitored using the IVIS 200 bioluminescence imaging system. In the first week after implantation, the migration of the implanted cells from the site of intraventricular injection toward the spinal cord depended on the presence of active EAE lesions (Fig. 2). Quantification of the bioluminescence in the EAE mice demonstrated that the initial signal at the site of deposition in the brain ventricle decreased whereas the signal in the spinal cord increased (Fig. 2A–D, G). No differences were observed between the migration of NSCs or Olig2-NSCs in the EAE mice, indicating a similar responsiveness to the signals from the spinal cord lesions. In control mice and in mice that had been implanted intraventricularly after recovery from the clinical attack of EAE relapse (late EAE, day 30, Fig. 1), no migration of implanted cells toward the spinal cord was detected (Fig. 2C, F, G). This illustrated that only active lesions produce attractants for the implanted cells. After a week, the level of bioluminescence activity in the spinal cord and the brain stabilized.

We analyzed the expression of the major chemokine receptors of NSCs, CXCR3 and CXCR4, both in undifferentiated NSCs and Olig2-NSCs and performed a chemotaxis assay for the chemokines CXCL9 and CXCL12. The results, depicted in Figure 3, did not reveal a significant difference between NSCs and Olig2-NSCs, confirming the similar migratory capacities of NSCs and Olig2-NSCs as observed in the implantation experiments.

NSCs and Olig2-NSCs Inhibit the Development of Acute EAE

Intraventricular injection of both NSCs and Olig2-NSCs induced a significant inhibition in the development of clinical EAE in FVB mice (Fig. 4) following the injection of NSCs and Olig2-NSCs on day 12, when mice exhibited a limp tail (clinical score of 1).

Immunohistochemical analysis of the spinal cord of FVB-EAE mice following intraventricular injections with labeled NSCs or Olig2-NSCs at days 20–23 revealed the presence of intraventricularly injected cells in the spinal cord (Fig. 5A–F). The posterior, lateral, and anterior funiculi of the EAE-spinal cord were highly cellular and contained numerous infiltrating cells (Fig. 5A). The luciferase-GFP-positive injected cells were detected among these cell infiltrations in the funiculus areas. Quantification of the number of implanted cells in these sections of spinal cord that were still present 10 days after injection revealed a slightly, but not significantly, higher survival rate for the Olig2-NSC in comparison to the NSCs. With double immunostaining, the identity of the differentiation direction of the injected cells was determined (Fig. 5G–H). The majority of the injected NSCs were still undifferentiated as revealed by their staining with anti-nestin antibodies, with only a small percentage of cells differentiating toward an OPC type (NG2 or RIP positive) and relatively few toward neurons (double-cortin staining) or astrocytes (S100 or GFAP staining). The majority of the injected Olig2-NSCs in the EAE spinal

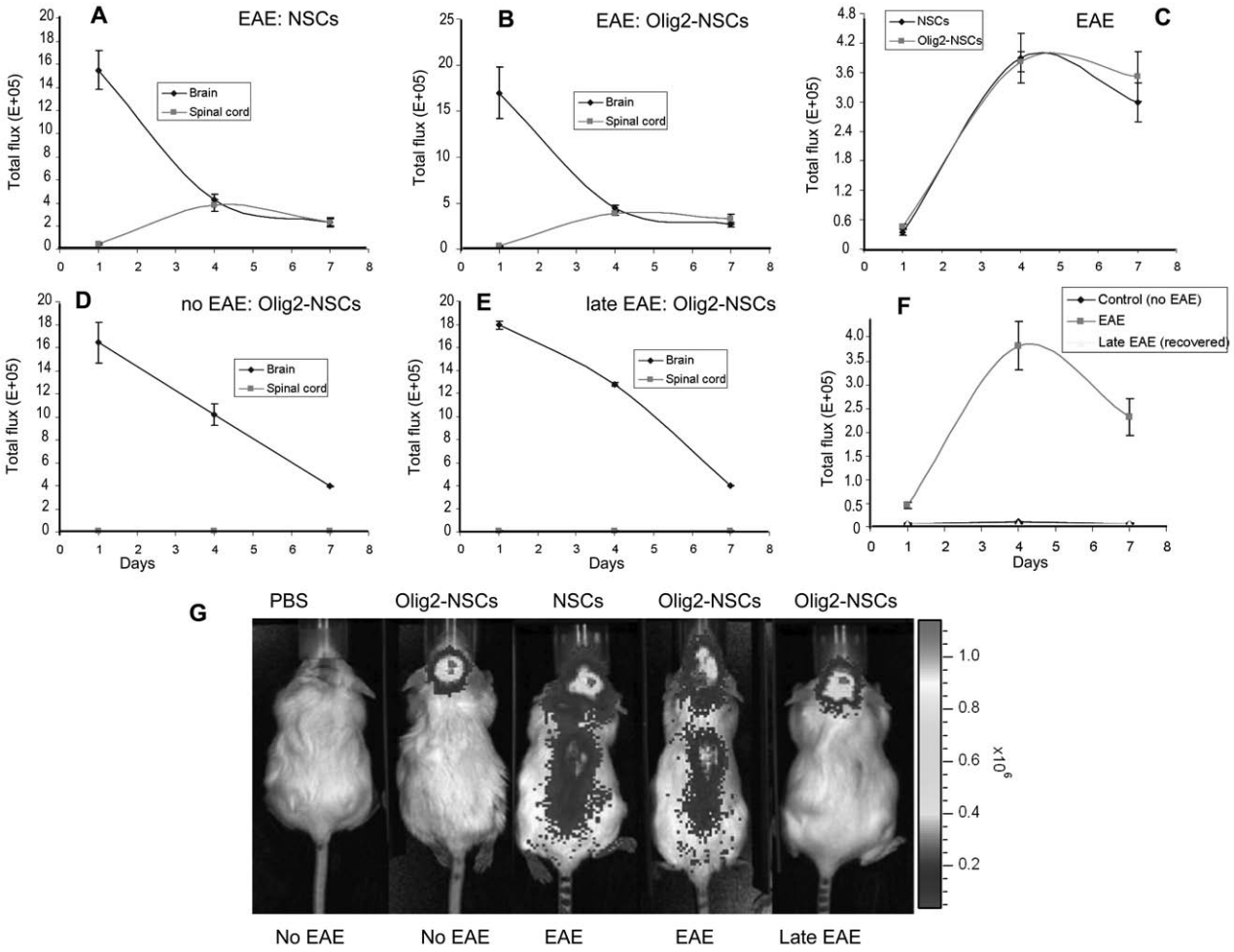

Figure 2. Distribution pattern of luciferase-labeled NSCs and Olig-NSCs in brain and spinal cord, as measured by bioluminescent intensity (total flux of photons), in the first week after their intraventricular implantation in EAE FVB mice. (A, B) A gradual decrease in bioluminescent activity in the brain and a concomitant increase in the spinal cord point to the migration of NSCs and Olig2-NSCs toward the spinal cord containing active EAE lesions. (C) Depicts in more detail the increase in bioluminescence activity in the spinal cord of EAE mice after intraventricular injections. (D, E) Intraventricular injection of luciferase-labeled NSCs and Olig-NSCs in control mice (no EAE) or at a late stage of EAE do not lead to an increase in bioluminescent intensity in the spinal cord. (F) Summarizing graph showing the distribution pattern in the spinal cord at the indicated conditions. (G) Examples of IVIS scans in control and implanted mice at 3 days after intraventricular injection. For each group: $n=5$ (±SEMs).

cord, however, developed into OPCs (NG2 positive) as was expected because of their OPC-primed state. However, none of these cells expressed MBP, indicating that none of them actually reached a mature myelinating stage. This is in line with the fact that demyelination rarely occurs in the primary acute disease episodes in this monophasic EAE model and so no new remyelinating cells are required.

EAE in Biozzi ABH Mice

Induction of EAE in the Biozzi ABH mice resulted in a chronic relapsing–remitting pattern of disease (Fig. 6A) in which the first attack (the acute phase) started between days 10 and 12, with a peak at day 22 and a return to normal scores around day 30. As in the monophasic course of FVB mice, the clinical signs in this acute form of EAE are the result of extensive cell infiltration and edema in the spinal cord. A second neurological attack (relapse) was observed 15 days later, reaching a plateau at score 3 from days 55 to 65, until the clinical score remitted to almost baseline scores around day 70 (Fig. 6B); the clinical signs in the relapsing disease in the Biozzi mice are initiated by cell infiltration, but they are particularly associated with subsequent demyelination, as has been extensively described before for this model (4).

NSCs and Olig2-NSCs Delay or Prevent the Onset of Relapses in Biozzi EAE Mice

To investigate the effect of intraventricular injections of NSCs and the OPC-primed Olig2-NSCs on the clinical course of EAE in the Biozzi mice, we injected both cell suspensions at day 12 at the first signs of clinical

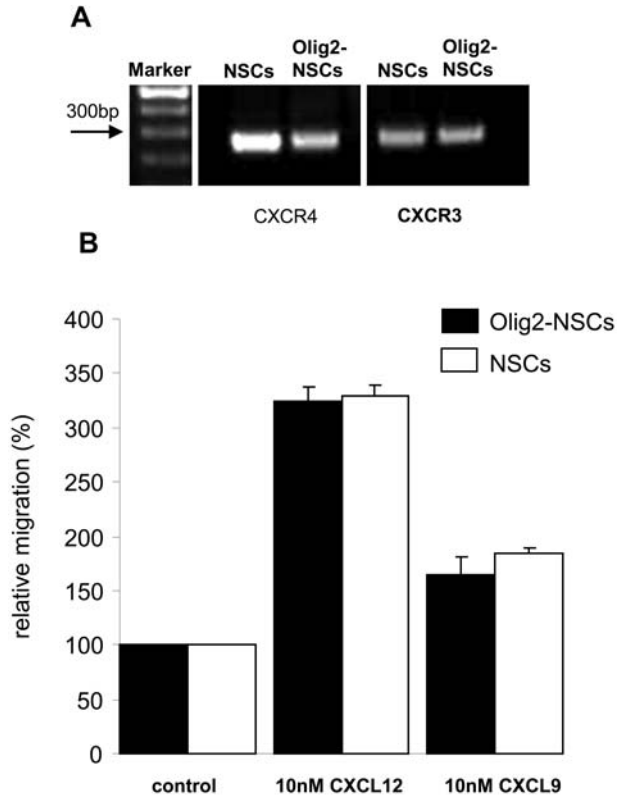

Figure 3. Chemokine signaling in NSCs and Olig2-NSCs. (A) RT-PCR analysis shows that NSCs as well as Olig2-NSCs express the major chemokine receptors CXCR3 and CXCR4. (B) Moreover, NSCs and Olig2-NSCs have an equal migratory response to the chemokines CXCL12 and CXCL9 in a chemotaxis assay. The data of the chemotaxis assay in (B) are presented as percentages of control migration ($n=3, \pm$SEM); control migration in response to neurobasal media is set to 100%.

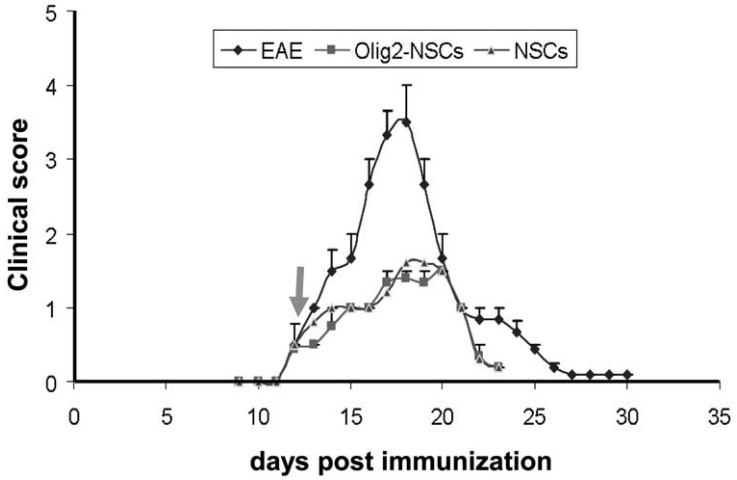

Figure 4. EAE disease course in FVB mice following stem cell transplantation. The intraventricular injection of NSCs ($n=5, \pm$SEM) or Olig2-NSCs ($n=5, \pm$SEM) at the beginning of EAE (arrow) blocks the development of clinical EAE; untreated disease course taken from Figure 1A (data generated for Figs. 1 and 4 were collected in one and the same experiment, at the same time).

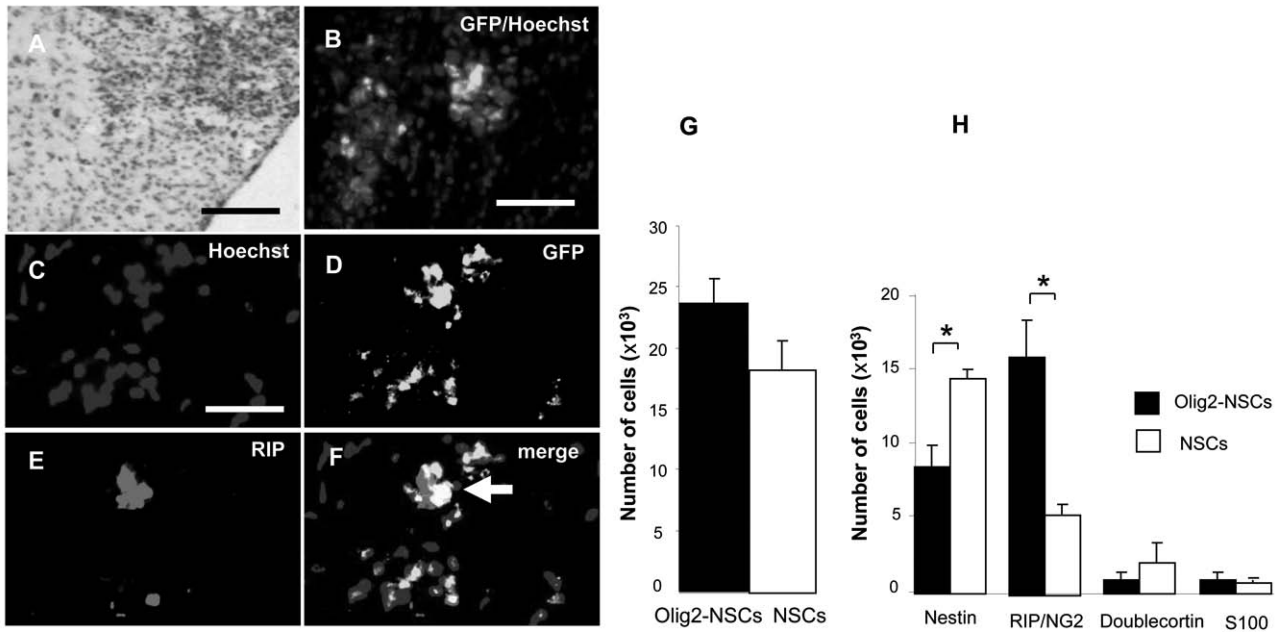

Figure 5. Immunohistochemical analysis of spinal cord of FVB-EAE mice after intraventricular injections with labeled NSCs or Olig2-NSCs. (A, B) Green fluorescent protein (GFP)-labeled cells have migrated from the intraventricular injection site in the brain to the spinal cord and are located in the lesions (GFP/Hoechst nuclear staining). (C–F). Double immunostaining for GFP and RIP shows examples of injected Olig2-NSCs that differentiated into oligodendrocyte precursor cells (OPCs). (G) The bar graph shows the number of intraventricularly injected Olig2-NSCs and NSCs that were found in the spinal cord of EAE FVB mice ($n = 5$, mean ± SD) (H) Quantification of the differentiation pattern of the injected NSCs and Olig2-NSCs found back in the spinal cord shows that a majority of the Olig2-NSCs differentiated into OPCs, whereas most of the NSCs stayed undifferentiated (nestin-positive) ($n = 5$, mean ± SD; $*p \leq 0.05$, Student's t test). Scale bars: 100 μm (for A, B) and 50 μm (for C–F).

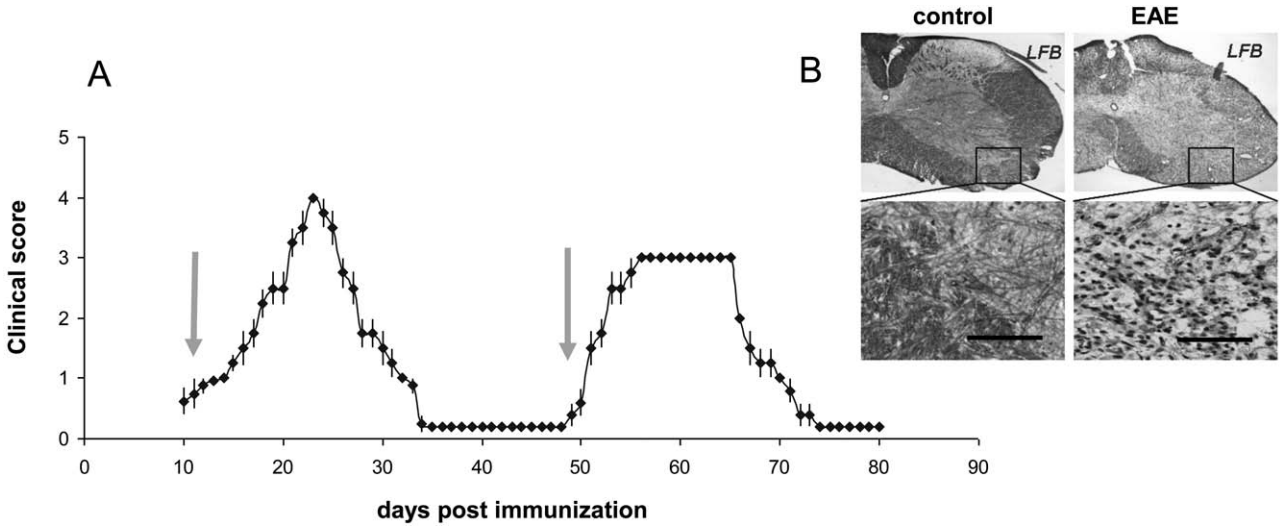

Figure 6. EAE disease course in Biozzi ABH mice. (A) The clinical scores of EAE in these mice ($n = 10$; ±SEMs) reveal a more chronic pattern with a primary response and remittance phase followed by a relapse approximately 50 days after immunization; the relapse pattern shows a typical extended flattened peak of clinical score. Arrows indicate the time points of intraventricular injections of NSCs and Olig2-NSCs. (B) Sections of spinal cord stained for Luxol Fast Blue (LFB) taken from control mice and EAE Biozzi mice at the peak of the relapse show demyelination in the funiculus white matter. Scale bar: 100 μm.

disease (Fig. 7). Like in FVB mice, both intraventricularly injected cell suspensions affected the clinical score in Biozzi mice with an even more dramatic inhibition of disease development, which resulted in the lack of neurological signs of EAE by day 20. We continued to monitor these Biozzi mice for the appearance of a relapse and surprisingly noted that this relapse was significantly delayed by approximately 10 days with the typical extended peak of paresis significantly shortened in case of NSCs injections; remarkably, in the case of Olig2-NSCs injections, relapsing disease was completely inhibited (Fig. 7).

Intraventricularly Injected NSCs Migrate Also to Active Relapse EAE Lesions

In order to investigate the migratory response of intraventricularly injected NSCs to the lesioned spinal cord in the relapse phase, luciferase or dragon green fluorophore-labeled NSCs and Olig2-NSCs were intraventricularly injected in Biozzi mice at the onset of the relapse, when mice exhibited a score of 1, about 50 days after immunization. Bioluminescence and fluorescence in vivo monitoring revealed that NSCs and Olig2-NSCs migrated from the site of injection toward the spinal cord lesions (Fig. 8). This indicated that these lesions in relapse produced sufficient chemotactic signals to attract the implanted cells.

NSCs and Olig2-NSCs Implanted at the Onset of Relapsing Disease Inhibit the Development of Clinical EAE

Next, we examined the impact of injecting NSCs and Olig2-NSCs during established EAE at the onset of the clinical relapse in Biozzi mice (Fig. 9). Like in the primary acute stage, both NSCs and Olig2-NSCs inhibited the development of clinical paresis to severe disability as observed in the untreated control EAE mice. When the clinical scores remitted and returned to 0.5 approximately 10 days after injection, the mice were perfused for immunohistochemical analysis (Fig. 10). Immunohistochemical analysis of the spinal cord of these mice revealed the presence of intraventricularly injected dragon green fluorophore-labeled cells in the more superficial regions of the posterior, lateral, and anterior funiculus of the spinal cord (Fig. 10A–F). Quantitative analysis of the presence, distribution, and differentiation pattern of the NSCs and Olig2-NSCs revealed similar patterns as described for NSCs and Olig2-NSCs injected at the onset of the acute EAE in the FVB mice (Fig. 10G, H); however, the total number of cells found in the spinal cord of Biozzi mice after injection at the onset of the relapse was almost double in comparison to the studies in FVB mice (Fig. 5G, H). Similar to the FVB mice, a majority of the injected Olig2-NSCs, in contrast to the undifferentiated injected NSCs, started to differentiate into early OPCs in the spinal cord at the relapse phase in Biozzi ABH mice. The rapid inhibitory effect on cell infiltration by the intraventricularly injected NSCs and Olig2-NSCs at the start of the relapse in the Biozzi mice prevented the occurrence of wide-scale demyelination responsible for the otherwise chronic clinical episode. However, in contrast to the NSCs, the Olig2-NSC-derived OPCs contributed to an indeed only limitedly required remyelination and maturated into oligodendrocytes. Electron microscopy revealed the presence of these injected Olig2-NSC-derived oligodendrocytes that contributed to myelin sheath formation (Fig. 11); these injected cells could be identified in electron microscopy sections by the large electron-dense particles of the dragon green fluorophores (Fig. 11A–E).

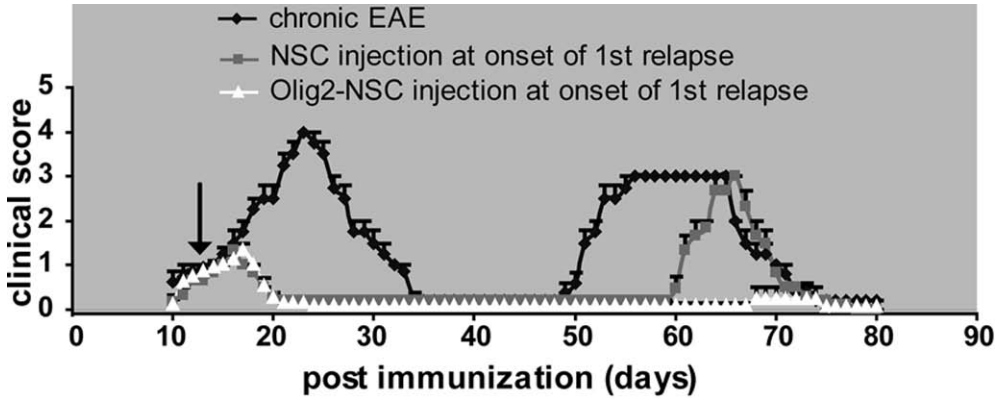

Figure 7. EAE disease course in Biozzi ABH mice after intraventricular NSCs and Olig2-NSCs injections. NSCs and Olig2-NSCs (both groups $n = 4$) injected intraventricularly at the onset of acute EAE (arrow) directly prevent the further development of clinical signs of EAE. Moreover, the injection of NSCs (squares) significantly delays the development of subsequent relapse and abolishes the occurrence of a typical extended score peak; the Olig2-NSCs injections (triangles) appear to completely prevent the occurrence of a relapse in Biozzi EAE mice (untreated disease course taken from Fig. 6A).

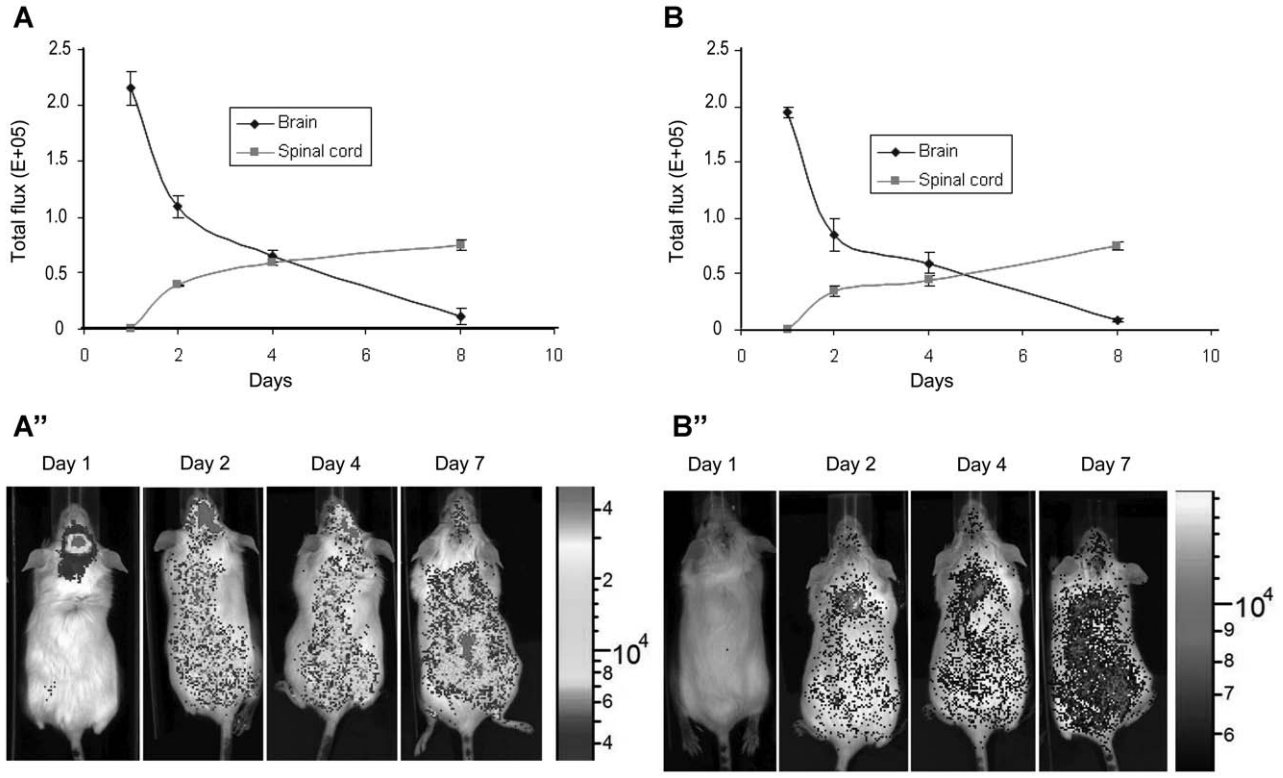

Figure 8. Distribution pattern of luciferase-labeled NSCs (A) and dragongreen fluorophore labeled Olig2-NSCs (B) in brain and spinal cord, as measured by bioluminescent or biofluorescent intensity (total flux of photons), in the first week after their intraventricular implantation in EAE Biozzi mice. (A) A gradual decrease in bioluminescent activity in the brain and a concomitant increase in the spinal cord point to the migration of NSCs toward the spinal cord containing active EAE lesions; (A") example of IVIS-bioluminescence scans taken from a Biozzi EAE mouse at days 1, 2, 4, and 7 after intraventricular injection. (B) A similar gradual decrease as in bioluminescence was seen in biofluorescent activity in the brain and a concomitant increase in the spinal cord reflecting the migration of Olig2-NSCs toward the spinal cord containing active EAE. For each group: $n=5$ (±SEMs).

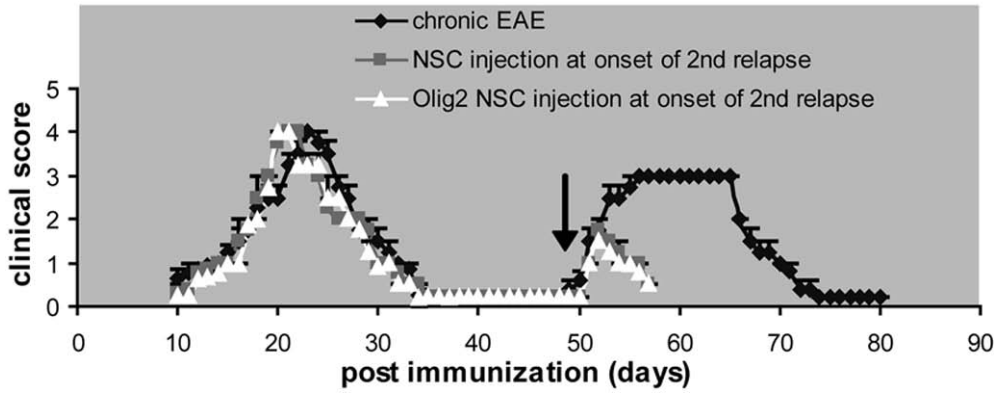

Figure 9. EAE progression and clinical scoring in Biozzi mice after the injection of NSCs and Olig2-NSCs at the onset of a relapse (arrow). Both types of cell injections (squares and triangles, $n = 4 \pm$ SEM for both groups) directly prevent the progression of a relapse and reduce the clinical score (untreated disease course taken from Fig. 6A).

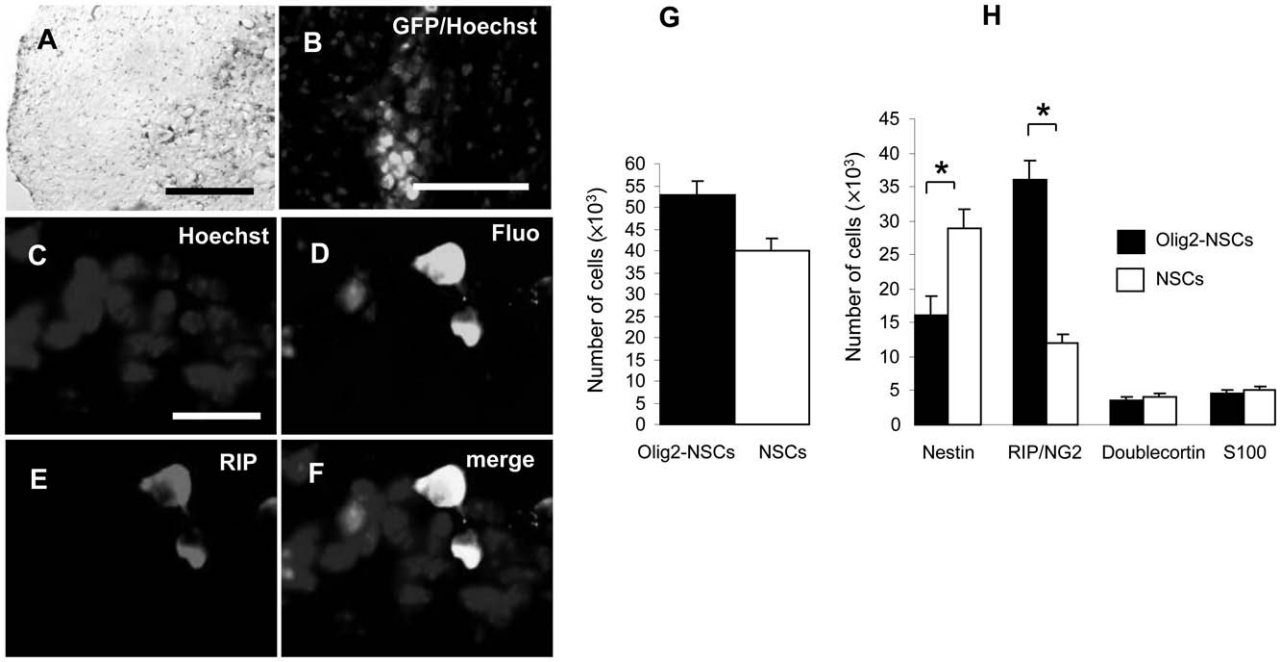

Figure 10. Immunohistochemical analysis of the spinal cord of Biozzi EAE mice that received intraventricular injections with labeled NSCs or Olig2-NSCs at the onset of the relapse. Spinal cord was collected at day 10 after injection (see Fig. 9). (A) Cresyl violet-stained section of Biozzi EAE spinal cord. (B) GFP-labeled cells have migrated from the intraventricular injection site in the brain to the spinal cord and are located in the lesions (GFP/Hoechst nuclear staining). (C–F) Double immunostaining for dragon green fluorescein (Fluo,) and RIP shows examples of injected Olig2-NSCs that differentiated into OPCs. (G) The bar graph shows the number of intraventricularly injected Olig2-NSCs and NSCs that were found in the spinal cord of EAE Biozzi mice ($n=3$, mean ± SD; $*p \leq 0.05$). (H). Quantification of the differentiation pattern of the injected NSCs and Olig2-NSCs in the secondary lesions in the spinal cord shows that a majority of the Olig2-NSCs differentiated into OPCs, whereas most of the NSCs stayed undifferentiated (nestin-positive) ($n=3$, mean ± SD; $*p \leq 0.05$). Scale bars: 100 μm (for A, B) and 50 μm (for C–F).

DISCUSSION

Neural stem cells (NSCs) have been reported to be effective as a therapeutic strategy for neurodegenerative disorders such as the inflammatory demyelinating and neurodegenerative disease multiple sclerosis (MS). In acute EAE, implanted undifferentiated NSCs have been shown to promote repair and functional recovery predominantly by releasing a milieu of both neuroprotective factors and anti-inflammatory molecules (11–13,24–27). In the present study, we investigated whether NSCs also exert this effect in chronic relapsing EAE, the animal model that mimics the relapsing–remitting form of MS more closely. In addition, we wanted to test whether priming these NSCs to become OPCs by transient overexpression of Olig2 (9,31) could further promote the repair process by contributing in remyelination activity.

Our results of intraventricular implantation of NSCs at the onset of acute EAE disease confirm previous observations that undifferentiated NSCs are able to reduce the clinical signs of EAE associated with the primary acute or chronic response to EAE. No obvious differences were observed between NSCs and OPC-primed NSCs (Olig2-NSCs), suggesting that remyelination activity was not significantly contributing to these effects during this acute phase. Similar effects were observed when NSCs or Olig2-NSCs were injected at the onset of a relapse in Biozzi EAE mice, which are generally considered to mimic established (chronic) neurological disease in MS patients the most closely. In addition, we found that NSCs or Olig2-NSCs injected intraventricularly at the onset of the very first signs of disease induced a delay or a complete inhibition, respectively, of the occurrence of a later relapse. These data suggest that transplanted NSCs may interfere with T-cell activity, B cell responses, or indeed microglia/macrophage activation at the onset of the relapse either at the local level in the spinal cord or at a more peripheral level, for instance, in the lymph nodes; extensive research is needed to elucidate the underlying cellular and molecular mechanisms.

Various studies have shown that forced expression of the transcription factor Olig2 in NSCs promote their differentiation into OPCs (9,21). Transient overexpression of Olig2 in NSCs primed these cells to become OPCs after stereotactic injection in the corpus callosum of cuprizone-fed mice, an animal model for demyelination. In contrast to control NSCs, Olig2-NSCs were able

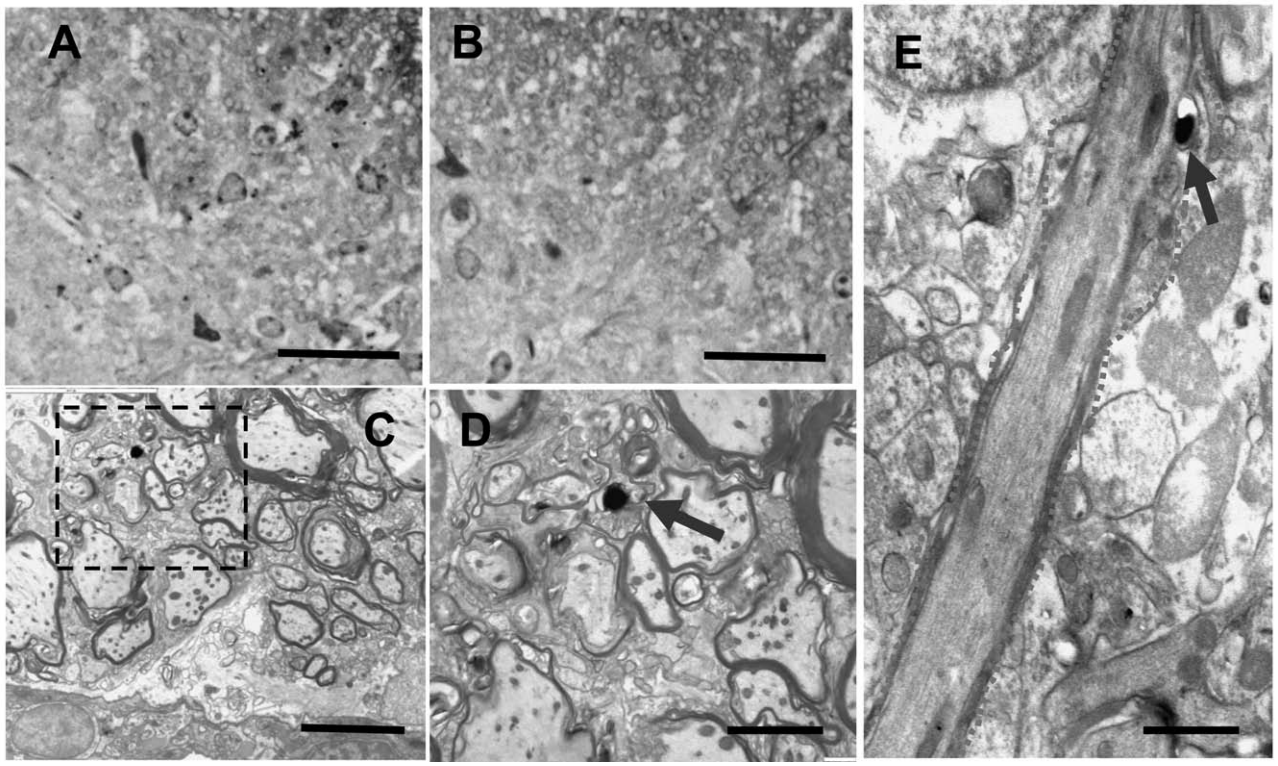

Figure 11. Electron microscopy of Biozzi spinal cord after cell injections at onset of relapsing EAE. (A) Toluidine-blue 1 μm section of a lesion site shows the presence of many implanted cells recognizable by the labeling with black fluorophore particles. (B) Outside the lesion site no grafted cells can be detected. (C) Among myelinated and unmyelinated fibers (part of) a grafted Olig2-NSC (area magnified in D; cell outlined) containing a large labeling particle (arrow) is located. (E) Example of an (particle labeled, arrow) implanted Olig2-NSC (cell contour in dotted lines) contributing to remyelination of an axon. Scale bars: 10 μm (in A and B), 2 μm (in C), and 1 μm (in D and E).

to survive, to differentiate into mature oligodendrocytes, and to remyelinate axons in the cuprizone mouse model for demyelination (9,31). Migratory activity of Olig2-NSCs was evident in these studies, but limited since they were stereotactically injected near the site of demyelination. In the present studies, we aimed to investigate the migration of NSCs and Olig2-NSCs after intraventricular injection toward lesions in the EAE mouse model for MS. It is well documented that NSCs express a wide variety of chemokine receptors (18,33,34) and the observed migration of NSCs toward lesions and, for instance, glioblastoma appear to depend on CXCR3/CXCL9 and CXCR4/CCL12 signaling (8,10,36). In order to check whether forced Olig2 expression did not alter the NSC-specific expression of chemokine receptors and change the migratory capacity, we verified the expression of the major chemokine receptors CXCR3 and CXCR4 in Olig2-NSCs and their response to the ligands CXCL9 and CXCL12. As illustrated by in vivo bioluminescence and biofluorescence imaging, NSCs as well as Olig2-NSCs migrated to the active EAE lesions in the spinal cord, apparently attracted by chemokines produced only by active lesions. In some injection experiments with the ABH mice, we labeled Olig2-NSCs with large dragon green fluorophore particles. The presence of these intracellular particles did not influence the migratory capacity of these cells to EAE lesions as was also previously demonstrated for NSCs containing similar-sized magnetic particles (6).

Intraventricular injection not only at the onset of the first acute phase but also at the onset of the first relapse phase resulted in a direct migration of both NSCs and Olig2-NSCs toward the lesioned sites in the spinal cord. Obviously, the mode of application is important for the migratory behavior of injected cells (32); intravenous injection of NSCs results within 2 min in their massive accumulation in the lung (28), whereas direct injection of cells in the spinal cord near a lesioned area only result in their limited migration into normal areas causing additional axonal damage (16). The presence of NSCs and Olig2-NSCs in the lesioned spinal cord directly induced a significant inhibition in the further development in the clinical score, confirming the findings of other EAE implantation studies (11–13,23–27). The mechanisms of this protective action have been ascribed to the production of a wide variety of trophic and immunomodulatory factors by NSCs that appear to reduce cell infiltration,

restrain dendritic cell function, and cause the selective death of reactive T cells (11,26,27). Most of the immunomodulatory interaction between the grafted NSCs and immune cells in our studies must have taken place at the spinal cord level since we were unable to trace intraventricularly injected NSCs back in peripheral organs, like spleen or lung; only sporadically a few injected NSCs could be detected in cervical lymph nodes a week after injection. We speculated that in particular the OPC-primed Olig2-NSCs would additionally contribute to the reduction of signs with supportive remyelination activity. Remyelination activity in the spinal cord lesions by the injected Olig2-NSCs was not detected in the acute lesions but only in the relapsing disease episodes in the Biozzi mice. Since the immediate effect of the intraventricularly injected NSCs and Olig2-NSCs on cell infiltration and inflammation apparently prevented wide-scale demyelination to occur in the relapse phases of EAE, the amount of required remyelination (and the contribution of Olig2-NSCs to that) was low accordingly. To really establish a more prominent contribution of Olig2-NSCs to myelin repair in EAE lesions, we would need to inject these cells at a later stage in the relapsing disease course, when demyelination indeed is a prominent component. However, such an experimental set-up (Olig2-NSCs injection in high score diseased animals) would currently face insurmountable objections by the local ethical committee for experimental animal research. Despite a similar anti-inflammatory action, we observed considerable differences in the survival and differentiation in the spinal cord lesions between the NSCs and the Olig2-NSCs: the survival rate of Olig2-NSCs was significantly higher, presumably due to the fact that most of them differentiated into OPCs, in comparison to control NSCs, where the majority maintained an undifferentiated state. In addition, it has been reported in some studies that Olig2 can support cell survival (11,35).

The most interesting finding of the present research is the fact that early injection of NSCs at the onset of the very first EAE signs of disease appears to delay and reduce the extent of a relapse and in case of Olig2-NSCs even completely prevent a relapse from occurring. Apparently, the presence of surviving injected NSCs and in particular NSC-derived OPCs in the spinal cord modify local conditions and/or instruct local cells (like microglia) resulting in a reduced invasion and/or activity of aggressive T cells. A role for the peripheral lymph node system seems unlikely since only very sporadically injected cells were detected in them. An instructive mechanism by secreted factors, similar to suggested for implanted bone marrow cells and mesenchymal stem cells (e.g., 5,14,19), seems more likely. It has been demonstrated that, in addition to the neurotrophic and anti-inflammatory factors already described for the NSCs (e.g., 11,15,26,27), stem cell-derived OPCs do produce significant amounts of chemokines and cytokines among which transforming growth factor β (TGF-β), interleukin (IL)-6 and IL-8 (37). These factors have been shown to reduce blood–brain barrier permeability and to reduce microglia and astrocyte activation; in particular, TGF-β has been shown to mitigate EAE through the induction of anergy and infectious tolerance in regulatory T lymphocytes (30). The mechanisms behind the effects of implanted NSCs and Olig2-NSCs are now the subject of extensive detailed research since they may be of considerable significance for a potential cell transplantation therapy for relapsing–remitting MS (RRMS) patients that aimed to suppress relapses and to prevent a transition toward the secondary progressive state.

ACKNOWLEDGMENTS: This research was supported by a grant of the Dutch Foundation MS Research, MS 04-554MS. We also acknowledge the support of the National Multiple Sclerosis Society, UK. We gratefully acknowledge the technical assistance by Ietje Mantingh-Otter and Freark Dijk.

REFERENCES

1. Amor, S.; Baker, D.; Groome, N.; Turk, J. L. Identification of a major encephalitogenic epitope of proteolipid protein (residues 56–70) for the induction of experimental allergic encephalomyelitis in Biozzi AB/H and nonobese diabetic mice. J. Immunol. 150:5666–5672; 1993.
2. Amor, S.; Groome, N.; Linington, C.; Morris, M. M.; Dornmair, K.; Gardinier, M. V.; Matthieu, J. M.; Baker, D. Identification of epitopes of myelin oligodendrocyte glycoprotein for the induction of experimental allergic encephalomyelitis in SJL and Biozzi AB/H mice. J. Immunol. 153:4349–4356; 1994.
3. Amor, S.; O'Neill, J. K.; Morris, M. M.; Smith, R. M.; Wraith, D. C.; Groome, N.; Travers, P. J.; Baker, D. Encephalitogenic epitopes of myelin basic protein, proteolipid protein, myelin oligodendrocyte glycoprotein for experimental allergic encephalomyelitis induction in Biozzi ABH(H-2Ag7) mice share an amino acid motif. J. Immunol. 156:3000–3008; 1996.
4. Baker, D.; O'Neill, J. K.; Gschmeissner, S. E.; Wilcox, C. E.; Butter, C.; Turk, J. L. Induction of chronic relapsing experimental allergic encephalomyelitis in Biozzi mice. J. Neuroimmunol. 28:261–270;1990.
5. Barhum, Y.; Gai-Castro, S.; Bahat-Stromza, M.; Barzilay, R.; Melamed, E.; Offen, D. Intracerebroventricular transplantation of human mesenchymal stem cells induced to secrete neurotrophic factors attenuates clinical symptoms in a mouse model of multiple sclerosis. J. Mol. Neurosci. 41(1):129–137; 2010.
6. Ben-Hur, T.; van Heeswijk, R. B.; Einstein, O.; Aharonowiz, M.; Xue, R.; Frost, E. E.; Mori, S.; Reubinoff, B. E.; Bulte, J. W. Serial in vivo MR tracking of magnetically labeled neural spheres transplanted in chronic EAE mice. Magn. Reson. Med. 57:164–171; 2007.
7. Buchet, D.; Baron-VanEvercooren, A. In search of human oligodendroglia for myelin repair. Neurosci. Lett. 456:112–119; 2009.
8. Carbajal, K. S.; Schaumburg, C.; Strieter, R.; Kane, J.; Lane, T. E. Migration of engrafted neural stem cells is mediated by CXCL12 signaling through CXCR4 in a viral

model of multiple sclerosis. Proc. Natl. Acad. Sci. USA 107:11068–11073; 2010.
9. Copray, S.; Balasubramaniyan, V.; Levenga, J.; de Bruijn, J.; Liem, R.; Boddeke, E. Olig2 overexpression induces the in vitro differentiation of neural stem cells into mature oligodendrocytes. Stem Cells 24:1001–1010; 2006.
10. Dziembowska, M.; Tham, T.N.; Lau, P.; Vitry, S.; Lazarini, F.; Dubois-Dalcq, M. A role for CXCR4 signaling in survival and migration of neural and oligodendrocyte precursors. Glia 50:258–269; 2005.
11. Einstein, O.; Fainstein, N.; Vaknin, I.; Mizrachi-Kol, R.; Reihartz, E.; Grigoriadis, N.; Lavon, I.; Baniyash, M.; Lassmann, H.; Ben-Hur, T. Neural precursors attenuate autoimmune encephalomyelitis by peripheral immunosuppression. Ann. Neurol. 61:209–218; 2007.
12. Einstein, O.; Grigoriadis, N.; Mizrachi-Kol, R.; Reinhartz, E.; Polyzoidou, E.; Lavon, I.; Milonas, I.; Karussis, D.; Abramsky, O.; Ben-Hur, T. Transplanted neural precursor cells reduce brain inflammation to attenuate chronic experimental autoimmune encephalomyelitis. Exp. Neurol. 198:275–284; 2006.
13. Einstein, O.; Karussis, D.; Grigoriadis, N.; Mizrachi-Kol, R.; Reinhartz, E.; Abramsky, O.; Ben-Hur, T. Intraventricular transplantation of neural precursor cell spheres attenuates acute experimental allergic encephalomyelitis. Mol. Cell. Neurosci. 24:1074–1082; 2003.
14. Gordon, D.; Pavlovska, G.; Uney, J. B.; Wraith, D. C.; Scolding, N. J. Human mesenchymal stem cells infiltrate the spinal cord, reduce demyelination, and localize to white matter lesions in experimental autoimmune encephalomyelitis. J. Neuropathol. Exp. Neurol. 69:1087–1095; 2010.
15. Hsu, Y. C.; Lee, D. C.; Chiu, I. M. Neural stem cells, neural progenitors, and neurotrophic factors. Cell Transplant. 16:133–150; 2007.
16. Hunt, D. P.; Irvine, K. A.; Webber, D. J.; Compston, D. A.; Blakemore, W. F.; Chandran, S. Effects of direct transplantation of multipotent mesenchymal stromal/stem cells into the demyelinated spinal cord. Cell Transplant. 17:865–873; 2008.
17. Hwang, D. H.; Kim, B. G.; Kim, E. J.; Lee, S. I.; Joo, I. S.; Suh-Kim, H.; Sohn, S.; Kim, S. U. Transplantation of human neural stem cells transduced with Olig2 transcription factor improves locomotor recovery and enhances myelination in the white matter of rat spinal cord following contusive injury. BMC Neurosci. 10:117; 2009.
18. Ji, J. F.; He, B. P.; Dheen, S. T.; Tay, S. S. Expression of chemokine receptors CXCR4, CCR2, CCR5 and CX3CR1 in neural progenitor cells isolated from the subventricular zone of the adult rat brain. Neurosci. Lett. 355:236–240; 2004.
19. Ko, H. J.; Kinkel, S. A.; Hubert, F. X.; Nasa, Z.; Chan, J.; Siatskas, C.; Hirubalan, P.; Toh, B. H.; Scott, H. S.; Alderuccio F. Transplantation of autoimmune regulator-encoding bone marrow cells delays the onset of experimental autoimmune encephalomyelitis. Eur. J. Immunol. 40(12):3499–3509; 2010.
20. Lin, Y. W.; Deveney, R.; Barbara, M.; Iscove, N. N.; Nimer, S. D.; Slape, C.; Aplan, P. D. OLIG2 (BHLHB1), a bHLH transcription factor, contributes to leukemogenesis in concert with LMO1. Cancer Res. 65:7151–7158; 2005.
21. Maire, C. L.; Buchet, D.; Kerninon, C.; Deboux, C.; Baron-Van Evercooren, A.; Nait-Oumesmar, B. Directing human neural stem/precursor cells into oligodendrocytes by overexpression of Olig2 transcription factor. J. Neurosci. Res. 87:3438–3446; 2009.
22. Paxinos, G.; Franklin, B. J. The Mouse Brain in Stereotaxic Coordinates, 2nd ed. Amsterdam, The Netherlands: Elsevier Academic Press; 2001.
23. Pluchino, S.; Gritti, A.; Blezer, E.; Amadio, S.; Brambilla, E.; Borsellino, G.; Cossetti, C.; Del Carro, U.; Comi, G.; 't Hart, B.; Vescovi, A.; Martino, G. Human neural stem cells ameliorate autoimmune encephalomyelitis in non-human primates. Ann. Neurol. 66:343–354; 2009.
24. Pluchino, S.; Martino, G. The therapeutic plasticity of neural stem/precursor cells in multiple sclerosis. J. Neurol. Sci. 265:105–110; 2008.
25. Pluchino, S.; Quattrini, A.; Brambilla, E.; Gritti, A.; Salani, G.; Dina, G.; Galli, R.; Del Carro, U.; Amadio, S.; Bergami, A.; Furlan, R.; Comi, G.; Vescovi, A. L.; Martino, G. Injection of adult neurospheres induces recovery in a chronic model of multiple sclerosis. Nature 422:688–694; 2003.
26. Pluchino, S.; Zanotti, L.; Brambilla, E.; Rovere-Querini, P.; Capobianco, A.; faro-Cervello, C.; Salani G.; Cossetti, C.; Borsellino, G.; Battistini, L.; Ponzoni, M.; Doglioni, C.; Garcia-Verdugo, J. M.; Comi, G.; Manfredi, A. A.; Martino, G. Immune regulatory neural stem/precursor cells protect from central nervous system autoimmunity by restraining dendritic cell function. PLoS One 4:e5959; 2009.
27. Pluchino, S.; Zanotti, L.; Rossi, B.; Brambilla, E.; Ottoboni, L.; Salani, G.; Martinello, M.; Cattalini, A.; Bergami, A.; Furlan, R.; Comi, G.; Constantin, G.; Martino, G. Neurosphere-derived multipotent precursors promote neuroprotection by an immunomodulatory mechanism. Nature 436:266–271; 2005.
28. Reekmans, K. P.; Praet, J.; De Vocht, N.; Tambuyzer, B. R.; Bergwerf, I.; Daans, J.; Baekelandt, V.; Vanhoutte, G.; Goossens, H.; Jorens, P. G.; Ysebaert, D. K.; Chatterjee, S.; Pauwels, P.; Van Marck, E.; Berneman, Z. N.; Van der Linden, A.; Ponsaerts, P. Clinical potential of intravenous neural stem cell delivery for treatment of neuro-inflammatory disease in mice? Cell Transplant. 20:851–869; 2011.
29. Scheper, W.; Copray, S. The molecular mechanism of induced pluripotency: A two-stage switch. Stem Cell Rev. 5:204–223; 2009.
30. Selvaraj, R. K.; Geiger, T. L. Mitigation of experimental allergic encephalomyelitis by TGF-beta induced Foxp3+ regulatory T lymphocytes through the induction of anergy and infectious tolerance. J. Immunol. 180:2830–2838; 2008.
31. Sher, F.; van Dam, G.; Boddeke, E.; Copray, S. Bioluminescence imaging of Olig2-neural stem cells reveals improved engraftment in a demyelination mouse model. Stem Cells 27:1582–1591; 2009.
32. Takahashi, Y.; Tsuji, O.; Kumagai, G.; Hara, C. M.; Okano, H. J.; Miyawaki, A.; Toyama, Y.; Okano, H.; Nakamura, M. Comparative study of methods for administering neural stem/progenitor cells to treat spinal cord injury in mice. Cell Transplant. 20:727–739; 2011.
33. Tran, P. B.; Banisadr, G.; Ren, D.; Chenn, A.; Miller, R. J. Chemokine receptor expression by neural progenitor cells in neurogenic regions of mouse brain. J. Comp. Neurol. 500:1007–1033; 2007.
34. Tran, P. B.; Ren, D.; Veldhouse, T. J.; Miller, R. J. Chemokine receptors are expressed widely by embryonic and adult neural progenitor cells. J. Neurosci. Res. 76:20–34; 2004.
35. Uchida, Y.; Nakano, S.; Gomi, F.; Takahashi, H. Differential regulation of basic helix-loop-helix factors Mash1 and Olig2 by beta-amyloid accelerates both differentiation

and death of cultured neural stem/progenitor cells. J. Biol. Chem. 282:19700–19709; 2007.
36. van der Meulen, A. A.; Biber, K.; Lukovac, S.; Balasubramaniyan, V.; den Dunnen, W. F.; Boddeke, H. W.; Mooij, J. J. The role of CXC chemokine ligand (CXCL)12-CXC chemokine receptor (CXCR)4 signalling in the migration of neural stem cells towards a brain tumour. Neuropathol. Appl. Neurobiol. 35:579–591; 2009.
37. Zhang, Y. W.; Denham, J.; Thies, R. S. Oligodendrocyte precursor cells derived from human embryonic stem cells express neurotrophic factors. Stem Cells Dev. 15:943–952; 2006.